



An Overview of Hydrogel-Based Bioinks for 3D Bioprinting of Soft Tissues

Soumitra Das and Bikramjit Basu*

Abstract | It has been widely perceived that three-dimensional bioprinted synthetic tissues and organ can be a clinical treatment option for damaged or diseased tissue repair and replacement. Conventional tissue engineering approaches have limited control over the regeneration of scaffold geometries and cell distribution. With the advancement of new biomaterials and additive manufacturing techniques, it is possible to develop physiologically relevant functional tissues or organs with living cells, bioactive molecules and growth factors within predefined complex 3D geometries. In this perspective, this review discusses how hydrogel-based bioinks can be used to mimic native tissue-like extracellular matrix environment, with optimal mechanical and structural integrity for patient-specific tissue regeneration, in reference to advanced bioprinting technologies to bioprint multitude of multicomponent bioinks. This review also summarizes various bioprinting techniques, the gelation and biodegradation mechanisms of hydrogel-based bioinks, the properties required for ideal bioink, challenges to design bioinks, as well as reviews the fabrication of 3D printed cardiac tissue, cartilages, brain-like tissue, bionic ear, and urinary system.

Keywords: 3D bioprinting, Bioink, Hydrogels, Tissue and organ fabrication

1 Introduction

Biofabrication is an emerging field in which complex biologically functional products are fabricated using extracellular matrix, growth factors, living cells and biomaterials.¹ Conventional biofabrication techniques, like electrospinning, solvent-casting, freeze-drying, particulate-leaching, injection moulding and gas-foaming can produce 3D scaffold-like geometry with a wide range of biomaterials.^{2–6} However, the scaffold architecture, pore geometry, spatial distribution, interconnectivity and reproducibility of the fabricated construct are limited. Most recently developed three-dimensional (3D) bioprinting approach has appeared as a novel biofabrication method, which can enable to develop highly complex tissue models with controlled porous geometry and high reproducibility.^{7,8} The 3D bioprinter is the device which can precisely seed the living cells within the biomaterials in a layer-by-layer approach using a

preprogrammed CAD model. One of the keys for success of bioprinting is the nature/characteristics of bioink, which comprise the printing media, within which living cells, nutrients and growth factors are mixed before or during printing.

Based on the cell deposition approach within the printed structure, bioprinting is classified into two major subgroups, scaffold-based approach and scaffold-free approach. The scaffold-based approach is the most widely explored technique, where living cells are loaded with a decellularized matrix component (synthetic or naturally occurring cell adhesive hydrogels) and are then bioprinted into a predefined structure.^{9,10} With the scaffold-free approach, cell aggregates or multicellular spheroids are deposited into a pre-printed 3D model/tissue fragments made with extracellular matrix component to improve the cellular interactions.^{11–14} Scaffold-based bioprinting takes a shorter printing time, compared

* Materials Research Centre, Indian Institute of Science, Bangalore, Karnataka 560012, India.
*bikram@iisc.ac.in

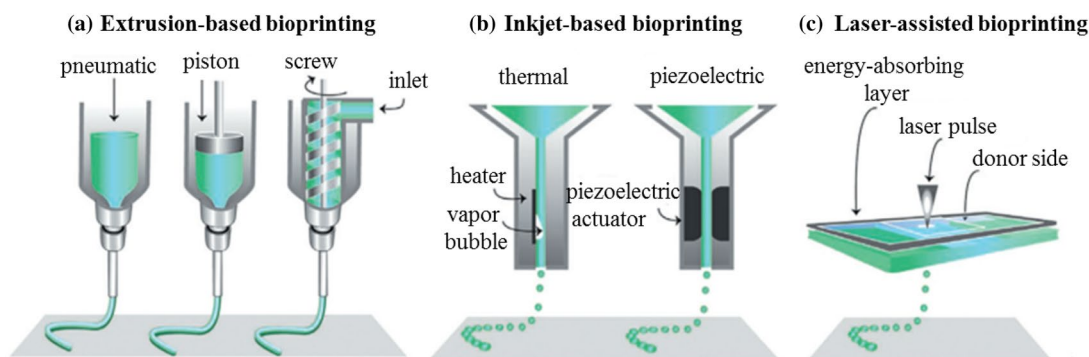


Figure 1: Schematic representation of the process physics involved in four different types of 3D bioprinting. **a** pneumatic, piston and screw-based extrusion bioprinting, **b** thermal and piezoelectric-based inkjet bioprinting **c** laser-assisted bioprinting ⁸.

to scaffold-free process. However, complete cell maturation can be obtained within a week for scaffold-free bioprinting, whereas scaffold-based process takes a much longer time.¹⁵

In case of scaffold-based bioprinting, the printing media is essentially a soft biomaterial in which living cells are loaded and can be deposited as a tissue-like replica, acquired from a computer-aided design model. An ideal bioink should have high bioprintability, the ability of in situ gelation during printing, printing fidelity, mechanical and structural stiffness, cytocompatibility with living cells, tissue regeneration properties, permeability of O₂, nutrients and metabolic waste and controlled biodegradability.^{7, 16–19} After bioprinting, the printed architecture should maintain the structural strength for a specific period of time and during tissue culture, should degrade in a controlled manner to replicate scalable functional tissue. The growth factors are the proteins or steroid hormones added within the bioink for proper cell differentiation, proliferation and tissue regeneration. Although bioprinting technology has been developed in recent decades, the fabrication of fully functional patient-specific organs has remained illusive. The primary issue that limits to construct a whole scalable organ is the unavailability of a suitable bioink. Conventional bioink materials are single-component hydrogels and do not have all of the properties of an ideal bioink. The present paper focuses on different bioprinting methods, choice of bioink materials, their physiological aspects and applications. This article also reviews various strategies to develop new-generation bioink materials for 3D bioprinting. Finally, this paper describes the future possibilities to build fully functional patient-specific tissues and organs using 3D bioprinting technology.

2 Scientific Approaches to 3D Bioprinting Technology

Biodegradable biopolymers are widely investigated in the area of 3D bioprinting. Living cells or cell aggregates can be encapsulated within the biopolymers and deposited in a preprogrammed manner to mimic native-like tissue structure.^{20–22} Several types of bioprinting approaches, such as extrusion-based,^{23, 24} inkjet-based,^{25, 26} and laser/light-assisted^{27, 28} bioprinting have been developed to fabricate the construct. Each of the printing strategies has some specific characteristic features, which control cell viability, and other fate processes during cell culture within the bioprinted construct.

Extrusion-based bioprinting (EBB) is a nozzle-based printing approach, where the printing process involves mechanical pressure to extrude the bioinks through the nozzle of a syringe in a controlled and continuous manner (Fig. 1a). The most promising features of EBB are the versatility of materials' choice over a wide range of bioink, and fabrication of chemically relevant tissues or organs with high accuracy. Most commonly, the extrudable bioinks are made up with the shear thinning biopolymers which helps to extrude the bioink. The printable biopolymers, termed as the hydrogels, are non-Newtonian fluids, where viscosity is reduced under shear stress. During extrusion, the mechanical pressure makes the entangled polymer chains aligned and reduces the viscosity of the bioink inside the nozzle and helps the living cells to survive. After printing, the hydrogel regains its viscosity due to zero shear and provides printing fidelity of the post-printed construct. Depending on the hydrogel's properties and cell characteristics, the mechanical pressure of an extrusion bioprinter can be pneumatic,

piston or screw-based. The extrusion pressure, nozzle diameter and printing speed of the extrusion bioprinter acutely affects the resolution, accuracy and overall structural fidelity of the printing construct. Optimisation of nozzle diameter is the main process parameter of the printer for a specific hydrogel. A nozzle with a small diameter for a viscous hydrogel requires high pressure, and a high extrusion pressure increases the shear stress to the cells. At a higher shear stress, the cells can damage, which can reduce cell viability after printing.^{29, 30} The pneumatic-based approach allows less cell damage due to less shearing during printing. The optimal nozzle diameter was found to be 150–300 μm of a Fab@Home 3D bioprinter where polyethylene-glycol diacrylate (PEGDA) and gelatin were used as a model hydrogel and porcine aortic valve interstitial cells (PAVIC) was considered as the model cell line.³¹ One of the major advantages of this technology is that highly viscous hydrogels with high cell concentration can be printed with a moderate speed. Furthermore, using a multi-head or co-axial head extrusion bioprinter, one can print multiple cell types using the same or different hydrogels within the same construct, such that a complex functional organ can be printed.

Inkjet bioprinting technology is based on the drop-on-demand strategies, where various biologics are encapsulated within hydrogel matrix, and the premixed bioink solutions are placed within the inkjet cartridge to be deposited dropwise through the inkjet printhead in a controlled manner (Fig. 1b). The bioink droplets can be generated via the application of either thermal energy^{26, 32} or piezo-electric impulses^{33, 34} to the bioink chamber. For thermal inject bioprinting, thermal energy produces small air bubbles, which create pressure pulse within bioink solution to eject the bioink droplets with different diameter. The droplet diameter depends on the temperature gradient, viscosity of the bioink and cell concentration. For piezoelectric inkjet bioprinting, a polycrystalline piezoelectric ceramic material converts the applied electric current to transient mechanical pressure, which creates bioink droplet to expel on building platform. The piezo-electric printhead can be either single or multiple. Multiple printheads can be used simultaneously to deposit various cell types in the same printed construct.³⁵ Sometimes it is convenient to use piezoelectric-based printhead because it can control the droplet volume more precisely compared to that of the thermal printhead. However, many researchers prefer thermal inkjet bioprinting over piezoelectric, since the usual working

frequency of piezoelectric printhead is within the range of 15–25 kHz, which can damage the cell membrane.²⁶

The printing resolution of this inkjet bioprinting is very high $\sim 50\text{--}300\ \mu\text{m}$.³⁶ However, this technique requires prolonged time, since droplet volumes are tiny within submicrometer diameter. The major drawback of this technique is that bioprinting is difficult when the viscosity of the hydrogel is high ($> 10\ \text{cP}$), and cell concentration is higher than $5 \times 10^6\ \text{cells/ml}$.³⁷ Cell clogging can occur in the nozzle due to cell aggregation or sedimentation, when the cell concentration is high. Furthermore, the hydrogels should have sufficient wettability and appropriate surface tension to pass through the cartridge and nozzle.

Laser-assisted bioprinting (LAB) is a nozzle free dispensing process, where bioink viscosity and cell concentration can be varied within a wide range without nozzle clogging. Without affecting the printing resolution, bioink viscosity can be varied between 1- and 300 mPa/s, whereas the cell concentration can be increased up to $1 \times 10^8\ \text{cells/ml}$ without occurring nozzle clogging.³⁷ The printhead setup comprises a ribbon, that is typically a laser transparent material made up with either glass slide or quartz. A laser-absorbing media (such as Ag, Au, Ti and TiO_2), is coated at the donor side of the ribbon and the cell-encapsulated hydrogels are sprayed on the laser-absorbing coating (Fig. 1c). The laser impulse focuses the absorbing media through the ribbon and the absorbing media evaporate with the creation of high local pressure on the bioink film. The vapour pressure of the absorbing media generates cavitation-like bubbles towards the bioink film. The expansion and collapse of the bubble creates a jet within the bioink layer which leads to the creation of the bioink droplets being transferred to the printing substrate.^{38, 39} The absorbing media also protects the hydrogel-encapsulated living cells from high-power laser pulse. Sometimes thick sacrificial metal layers are used instead of the absorbing medium. This layer shows rapid thermal expansion to expel small volumes of bioink from ribbon to the substrate. The process parameters of the LAB are the intensity and pulse duration of the laser radiation, diameter of the focused beam, viscosity and surface tension of bioink, and substrate properties. Besides so many advantages of the LAB, there are several drawbacks including continuous vaporisation of the absorbing media that contaminates the printed substrate. In LAP, the sprayed layer is very thin, which can dry quickly on the ribbon surface before printing.⁴⁰ Furthermore, cell

spreading onto the ribbon associated with random cell distribution occurs, which leads to non-uniform cell printing.

3 Hydrogel-Based Bioinks

Hydrogels are the most suitable material to mimic the native tissue structure using the 3D bioprinting method. Hydrogels are the crosslinked polymeric substances, which can absorb a large volume of water compared to their original dry weight (up to 1000 times) without dissolving in the medium.⁴¹ The hydrophilic functional groups present in their monomer unit are capable of restoring the absorbed water in the 3D network through hydrogen bonding. Growth factors and nutrients can be delivered with water to the hydrogel network to imitate extracellular matrix environments of the body tissue.⁴² The chemical and mechanical properties of biocompatible hydrogels can be precisely tailored in such a way that specific cellular interaction can happen within the printed cells so that cells can proliferate during tissue culture. Moreover, some of the hydrogels have specific cell-binding sites, which facilitate to bind the printed cells for spreading, growth and differentiation.⁴³

Bioprintable hydrogels can be classified into two groups: naturally derived hydrogels and synthetically derived hydrogels. The most frequently reported natural hydrogels are collagen, fibrin, hyaluronic acid, alginate, agarose, chondroitin sulfate, Matrigel, gellan gum, gelatin and chitosan, and among them, collagen, fibrin and gelatin have inherent signalling molecules for cell adhesion.⁴⁴ On the other hand, the familiar synthetically derived hydrogels are poly(ethylene glycol) (PEG), Pluronic®, polyanhydrides, poly(aldehyde guluronate), poly(vinyl alcohol) and poly(propylene fumarate).⁴⁵ Naturally derived hydrogels are the most common hydrogel materials used in tissue engineering applications due to their excellent bioactivity, and their molecular sequences, which are similar to the ECM of natural tissue. However, due to the limited mechanical strength and rapid biodegradable properties, natural hydrogels cannot afford the printing construct alone. Therefore, hybrid bioinks, derived from natural and synthetic hydrogels, have been developed to overcome the inadequacy of bioprinting.

3.1 Crosslinking Mechanism of Hydrogels

Hydrogel material possesses a three-dimensional network structure which is hydrated in an

aqueous medium. The term “network” implies the presence of crosslinking between the hydrophilic polymer chains. The crosslinking phenomenon of hydrogel molecules is called gelation. Hydrophilic polymers at a low to moderate concentration behave like a Newtonian fluid. However, the crosslinked molecules, termed as hydrogels, exhibit viscoelastic nature in aqueous solution.⁴⁶ Bioprintable hydrogels should have viscoelastic nature and quick gelation properties. After bioprinting, the individually printed layer must be crosslinked to develop the structural and mechanical integrity within the printed construct. Various crosslinking methods have been reported in the literature. Biodegradable and bioprintable hydrogel crosslinking should be done in physiological conditions and the gelation mechanism can be driven by chemical (through covalent bonding), physical (reversible interaction) and enzymatic crosslinking.

Physical crosslinking is one kind of gelation process, where the polymeric chains can be efficiently crosslinked without the formation of any covalent bonding. Since the crosslinking occurs through non-chemical interaction and no exogenous agent is used, there is no chance of cytotoxicity within the printed construct.⁴⁶ There are several reported mechanisms for physical crosslinking, such as ionic interaction, hydrophobic and hydrophilic interaction, self-assembly mechanism, stereo-complexation and thermal crosslinking.^{9,45–47}

Ionic crosslinking happens due to the electrostatic interaction between opposite charges. Bioink can be blended with multivalent ions or electrolyte solution, which is oppositely charged with the functional groups present in hydrogel chains. The blending ions can electrostatically attract the polymer chain and form crosslinked hydrogel network. Interestingly, for ionic crosslinking, the presence of ionic groups in the polymer chains is not necessary. Ionic crosslinking of alginate is a well-known example in 3D printing. Alginate consists of mannuronic and glucuronic acid in its polysaccharide chain and can form hydrogel using calcium ions at room temperature and physiological pH.⁴⁶ Another example of ionic crosslinking is that of chitosan-based hydrogels, which can be crosslinked using glycerol-phosphate disodium salt at 37 °C.⁴⁸

Hydrogels can involve physical gelation through hydrophobic interaction or hydrogen bonding interaction. This type of physical bonding depends on temperature and rheological changes. Some hydrogels exhibit physical gelation at a lower temperature due to ordered chain

conformation and upon heating, display random coil conformation. At lower temperatures, hydrogel molecules form a crosslinking network by hydrogen bonding with absorbed water. These hydrogels are thermosensitive, and gelation occurs at physiological temperature. The physical crosslinking of hydrogels can be of the stereocomplex type. When oligomers with opposite chirality, such as D- and L-lactic acid, are coupled with hydrophilic polymer chains, hydrogels are formed through stereocomplexation.⁴⁹ For example, polyethylene glycol can form triblock copolymer with poly(D-lactic acid) and poly(L-lactic acid) such as PLLA-PEG-PLLA and PDLA-PEG-PDLA. The blend of those two triblock copolymers can be crosslinked through stereocomplexation.⁵⁰

Chemical crosslinking involves covalent bonding between the polymer molecules. Since the covalent bonds are stronger compared to the physical bonding, mechanical strength of the printed structure should be higher after gelation. For chemical crosslinking, exogenous chemical agents termed as photo-initiators are added. In the presence of photo-radiation, the initiators form reactive free radicals through unimolecular bond cleavage. The free radicals promote covalent bonding between two polymer chains at the point of unsaturation. The photoinitiators can form undesirable reaction products, which leads to cytotoxicity and reduced cell viability.⁴⁶ Researchers are trying to develop biocompatible photo-initiators, which can overcome the cytotoxic issue. For 3D bioprinting, a UV curing head is used to cure each printed layer. The common wavelength used to cure the hydrogels is 365 nm or 405 nm. The exposure time of UV is an important feature during gelation since long time exposure can damage the cell's DNA. There are several photo-initiators commercially available for hydrogel gelatins such as Eosin Y,⁵¹ Irgacure 2959,⁵² LAP,⁵³ VA-086,⁵⁴ TPO,⁵⁵ Biokey⁵⁶ and DPPO.⁵⁷ The degree of crosslinking depends on the concentration of photo-initiator used within bioink. Although at a high initiator concentration, the mechanical strength of the printed construct increases, a longer time is required for hydrogel degradation. The conventional photoinitiators (Irgacure 2959, LAP) are used to initiate the polymerization in UV wavelength, which may either reduce cell viability or cause mutagenesis. Therefore, visible light-based photoinitiators (Eosin) can be used to avoid the cell damage and cytotoxicity.^{58, 59}

There are some specific enzymes which can crosslink biodegradable polymers through an enzymatic reaction. This mechanism is the

most cytocompatible process, since no exogenous reagents are used. For tissue engineering, fibrin is the most popularly used natural hydrogel, which undergoes enzymatic crosslinking.⁶⁰ Sperinde et al. reported that polyethylene glycol could enzymatically be crosslinked in the presence of transglutaminase enzyme in the aqueous solution of PEG-Qa and poly(lysine-co-phenylalanine).⁶¹ The γ -carboxamide groups of PEG-Qa and the ϵ -amine groups of poly(lysine-co-phenylalanine) yield an amide linkage between the polymer chains, accelerated with transglutaminase. There are several reported articles, where hyaluronic acid was enzymatically crosslinked for tissue engineering applications.^{62–65} Erica et al. revealed that peptide hydrogels can undergo enzymatic cross-linking. They reported that a multidomain peptide (MDP) contains four lysine residues and can be crosslinked using either lysyl oxidase or plasma amine oxidase.⁶⁶ Sanskrita et al. reported the enzymatic crosslinking of silk fibroin-gelatin (SF-G) bioink, where human nasal inferior turbinate tissue derived mesenchymal progenitor cells (hTMSCs) were encapsulated within the bioink and mushroom tyrosinase was used as the crosslinking enzyme.⁶⁷ The silk and/or gelatin consists of tyrosine residues which are oxidized into o-quinone through tyrosinase enzyme (Fig. 2). The o-quinone molecules can either generate free radicals, which are crosslinked with other o-quinone moiety or react with amino acid residues of silk fibroin and gelatin. The bioink concentration was optimized using 8% (w/v) autoclaved SF solution and 15 wt% ethanol sterilized gelatin powder. It was observed that the gelation kinetics of the bioink (8SF-15G) depends on both tyrosinase concentration and temperature. At a tyrosinase concentration of 300 units, the gelation rate was slower compared to the 500 unit tyrosinase concentration. At the temperature below 10 °C, no gelation occurred because at a lower temperature, the tyrosinase enzyme remained inactive. However, at 37 °C, the gelation mechanism started within 15 min and complete crosslinking appeared after 30 min. Although, there are several advantages of enzymatic crosslinking, the major challenge is the unavailability of a specific enzyme for the specific hydrogels to be crosslinked. Furthermore, optimization of enzyme concentration and printing temperature is necessary to execute the rapid gelation mechanism of the 3D printed hydrogel construct.

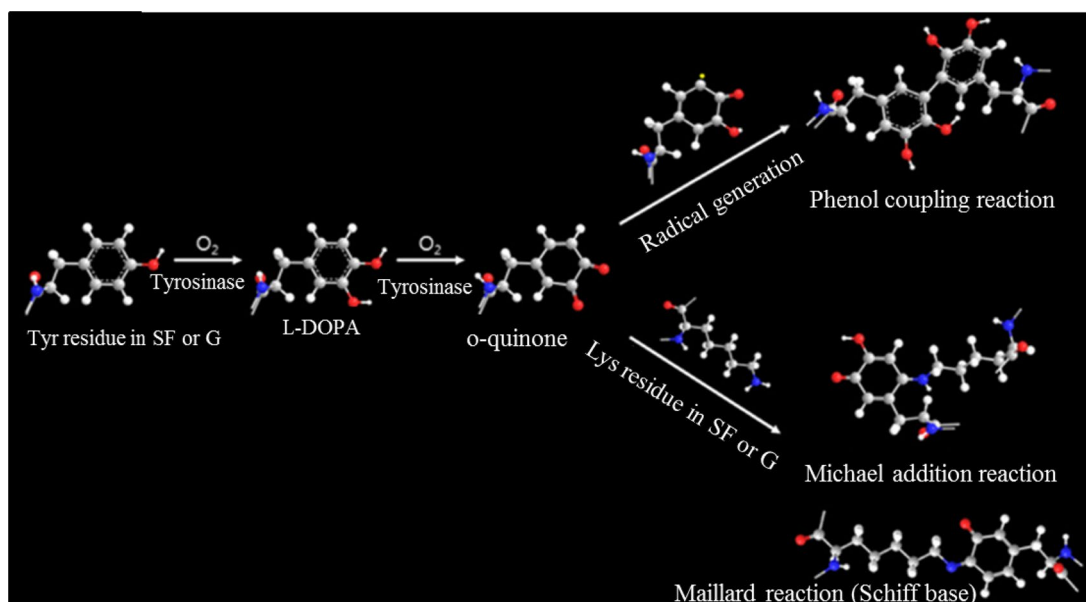


Figure 2: Three major steps involved in the in situ crosslinking mechanism of silk fibroin–gelatin bioink. Tyrosinase enzyme oxidizes the tyrosine residues of silk and/or gelatin into o-quinone moiety, which can either undergo free radical crosslinking with other o-quinone molecules or react with the amino acid residues of biopolymer chains⁶⁷

3.2 Hydrogel Degradation Mechanism

After bioprinting, the degradation of the hydrogel construct is necessary for proper cell differentiation during tissue culture. Although the mechanical support of the printed structure is essential for printing fidelity, the deterioration of the structure in a controlled manner is equally crucial for tissue regeneration. During cell differentiation, microvascular networks are formed within the tissue and to achieve patient-specific native-like organ. Besides, adequate oxygen and nutrients should be delivered, to the cells and metabolic wastes have to be removed from the hydrogel networks. For the successful operation of this process, the rate of hydrogel degradation should be similar to the cell differentiation rate. Several approaches have been developed to degrade the bioprinted hydrogel structure. Each bioprintable hydrogel possesses an inherent biodegradation property with cell differentiation. However, for controlled biodegradation, sometimes chemical modification is needed. For example, alginate is a bioinert (lack of cell adhesiveness) natural hydrogel. It shows limited and uncontrollable biodegradation properties under normal conditions. Chemical modification of alginate through oxidation altered the degradation property, which varies with the percentage of oxidation to the alginate molecules.⁶⁸ Jia et al. used periodate as the oxidizing agent of alginate, and the percentage (w/w) of oxidation

was varied, such as 1%, 3%, 5% and 10%. It was shown that for 10% oxidized alginate structure, there was almost complete fracture after 10 days of culture.⁶⁹ The ionically crosslinked hydrogel network can be degraded in the presence of chelating agents. For example, alginate-based hydrogels are physically crosslinked with calcium ions, and due to the low level of released calcium ions, the bioprinted construct showed slow degradation.⁷⁰ However, in the presence of sodium citrate, the citrate ions form a chelated complex with calcium ions, and after removal of calcium citrate, the alginate matrix dissolves within the tissue culture media.⁷¹ The concentration of the sodium citrate solution can control the degradation rate. It was reported that when the citrate to alginate molar ratio is 1000%, the whole printed construct of a hydrogel made with alginate/gelatin/collagen can be dissolved within 50 min (Fig. 3).¹⁶ The degradation rate of the hydrogel construct can be tailored using cell-responsive sites. For example, chitosan-based hydrogels show biodegradability with cell proliferation, when matrix metalloproteinase is used as the cell responsive site.^{72, 73} Synthetic hydrogels can provide superior mechanical properties of the bioprinted structure. However, the lack of cell response limits its use in bioprinting. Therefore, synthetic hydrogels are conjugated with various substances to improve biodegradability. For example, gelatin methacrylate (GelMA)

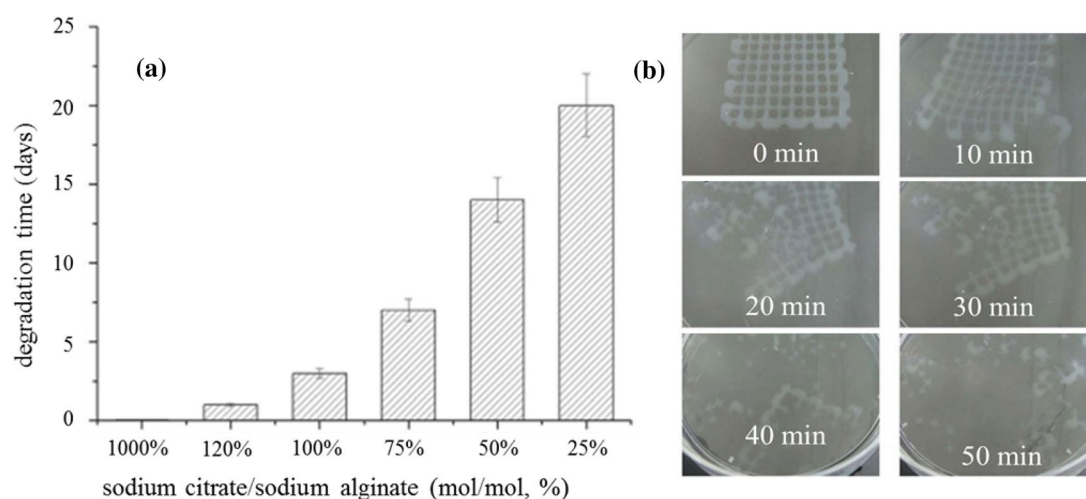


Figure 3: **a** Relation of the scaffold degradation by altering the mole ratio of sodium citrate to sodium alginate (C/A), **b** degradation of the printed scaffold with time, where the mole ratio of C/A is 1000%¹⁰

can be incorporated with PEG to improve cell attachment through their arginine–glycine–aspartic acid (RGD) sequences and improve biodegradability.⁷⁴

4 Property Requirement for Bioink Formulation

For scaffold-based 3D bioprinting, the bioink should have ideal biological, physicochemical, rheological and mechanical properties to construct native-like artificial tissue or organ (Fig. 4). One of the crucial aspects of hydrogels using for 3D bioprinting is the suitable rheological parameters, which determine the printability. Most of the hydrogels show a decrease of viscosity under shear stress. This behaviour of hydrogels helps to avoid nozzle clogging in the extrusion or inkjet process. Shear-thinning hydrogels possess a high zero shear viscosity, which provides excellent printing fidelity of the construct. A perfect shear-thinning hydrogel with desired viscosity can maintain the architectural integrity immediately after bioprinting. The printability of bioink depends on the concentration, hydrophilicity, surface tension, self-crosslinking ability of the hydrogel, cell density and surface properties of the printer nozzle. The printability and viscosity of the hydrogel determine the printing resolution, which refers to the precise architectural organisation of the native tissue. Furthermore, to create an ideal ECM-like microenvironment, the pore volume, shape, interconnectivity and distribution are the critical parameters. Pore interconnectivity allows the diffusion of O₂, nutrients and

metabolic products during proliferation.⁷⁵ The viscosity of the solution depends on the hydrogel concentration and density of the encapsulated cells. At a low solution viscosity, the printability is high, but the mechanical stability of the printed structure is inferior.⁷⁶ Besides, the cell reliability decreases at higher bioink viscosity, since a higher printing pressure is required to extrude. Various strategies have been taken to print high viscous bioinks in extrusion bioprinting. For example, when the extrusion bioprinting temperature increases from 20 to 37 °C, the viscosity of GelMA encapsulated hepatocarcinoma cells decreased from 10 to 0.01 Pa.s.⁵⁴ Moreover, for the same bioink, the viscosity should be changed with the printing technology. Cell viability within the printed bioink depends on hydrogel type and concentration, the interaction between cells, bioprinting modality, rate of hydrogel degradation and post-encapsulation time. A low concentration of hydrogel is more suitable for cell proliferation; however, the mechanical properties and fidelity is superior, when the hydrogel concentration is high. A highly concentrated hydrogel consists of densely packed polymer networks, which hinder cell proliferation and migration. Furthermore, tissue regeneration cannot be possible without cell spreading.⁹ Iliyana et al. reported that the cell spreading of human adipose tissue-derived mesenchymal stem cells (hAD-MSCs) depends on the critical hydrogel concentration of semi-synthetic gelatin-methacrylate. The hAD-MSCs are not supportive of cell spreading, when the concentration of GelMA is higher than 5%.⁷⁷ In the same article, they showed that



Figure 4: Schematic of the spectrum of properties required for ideal bioink formulation in 3D bioprinting ^{19, 116}

cell spreading also depends on the degree of functionalization (methacrylation) of both type A and B gelatin. The crosslinking density of the hydrogel network is an important parameter to determine the structural characteristics, mechanical properties, swelling ratio and permeability of the nutrients and metabolic waste. As the crosslinking density increases, the space between the macromolecular polymer chains decreases. Therefore, the mechanical strength of the printed construct is improved. However, the equilibrium swelling ratio and molecular diffusivity are reduced to a large extent.⁷⁸ As mentioned earlier, the bioink should possess excellent cell attachment properties with their characteristic chain sequence so that several biomolecules and biochemical signals are transferred within the printed cells.

Sometimes, it is necessary to modify the functional groups of the polymer chains to create cell attaching sites to improve cell–hydrogel interactions.⁷⁹ The biodegradation rate of the printed structure should match with the proliferation of the cell so that the ECMs of the cell can replace the biodegrading construct. Moreover, after degradation, the biodegrading product should not create any harmful impact to the regenerated tissues. Commercially, bioinks are developed based on their requirements of application. For specific tissue regeneration or specific cells' encapsulation, the hydrogel properties should ideally match with the printed cell, such that the scalable functional tissues can be fabricated. Besides the above-discussed features, the hydrogels should have some additional requirements, such as industrial

scalability, quick availability, economic feasibility and immunological compatibility, *in vivo*.

5 Biofabrication Window for Advanced Bioink

The application of 3D bioprinting to fabricate specific functional cellular or extracellular components can mimic physiologically relevant native tissues or organs. In such a context, the primary intention of bioprinting is to develop an extracellular microenvironment such that encapsulated cells can differentiate within the 3D printed construct. During cell differentiation, matrix remodelling and ECM synthesis, excellent cell–cell and cell–ECM interaction is required for appropriate cell signalling. Therefore, the selection of an ideal biomaterial is the primary step for successful bioprinting. Some of the naturally and synthetically derived known biopolymers have already been mentioned. The printable biopolymers are the hydrogels, which should have the properties including cytocompatibility, viscoelasticity, shear-thinning, rapid gelation kinetics, high swelling ratio, printing fidelity, the diffusivity of nutrients and metabolic products, and biodegradability. The traditional approach to formulate new bioink is to reflect from the biological point of view. Therefore, first of all, the bioink should possess cytocompatible hydrogels, which should have a high swelling ratio to generate an aqueous 3D microenvironment similar to that of the natural ECM. The advantage of natural biopolymers is their biocompatibility, which provides more cell-friendly microenvironments. On the other hand, 3D printed constructs with high printing fidelity are obtained from synthetic hydrogel-based bioinks. However, most of the synthetic hydrogels do not have active cell-binding sites and create inert microenvironments, which results in low cell viability. Therefore, several bioactive molecules, such as growth factors, therapeutic drugs and peptide sequences are incorporated or grafted with the synthetic hydrogel networks.⁹ Most of the traditional hydrogels are invented from either single-component natural or synthetic hydrogels. However, none of them can attain all of the required physical and biological properties near to the ideal bioink. The biofabrication window for 3D printing is an abstract idea for the traditional hydrogels which belong to the suboptimal state between the printing fidelity (fabrication window) and cytocompatibility (cell culture window).¹⁹ For the fabrication of patient-specific complex tissues or organs, the printing resolution and fidelity should be very high.

Moreover, for tissue regeneration, the hydrogel construct should provide the appropriate ECM-like microenvironment for cell differentiation, migration and proliferation. High resolution and fidelity of the printed construct can be achieved through the increment of hydrogel stiffness, which is associated with the concentration and crosslinking density.⁷⁸ Although the mechanical stiffness increases the shape fidelity, cell differentiation, migration and proliferation rates decrease. Therefore, the biofabrication window for traditional bioinks compromises the properties between structural integrity and cytocompatibility (Fig. 5). However, the advanced bioinks can simultaneously satisfy these two opposing requirements, and the biofabrication window can be shifted towards the ideal bioinks. Advanced bioinks are within the future biofabrication window where the fabricated bioinks should possess high printing fidelity with cytocompatibility.⁸⁰

Several novel strategies have been developed to fabricate advanced bioinks, which ensure high shape fidelity and maximal cell spreading. The traditional bioinks, fabricated with the single-component hydrogels, compromise the properties between biocompatibility and shape fidelity. The advanced bioinks are the multicomponent biomaterials that consist of more than one type of hydrogel, functionalized biomolecules, biocompatible organic and inorganic nanomaterials or microcarriers. Chimene et al. classified the advanced bioinks into four groups, such as multimaterial bioinks, interpenetrating network (IPN) bioinks, nanocomposite bioinks and supramolecular bioinks.¹⁹ Among the bioinks, gelatin methacrylate (GelMA) based hydrogels are extensively used as the bioink in the advanced 3D bioprinting domain during the past few years (Table 1). Gelatin is the denaturalized form of collagen, which is the primary component of natural ECMs. GelMA is a semi-natural hydrogel, which can be synthesized via the chemical modification (methacrylation) of gelatin and can form physical gel through thermo and photoresponsive mechanisms. The crosslinking density, as well as stiffness of GelMA, depends on the degree of crosslinking that can be optimized through the degree of methacrylation of gelatin and the concentration of photoinitiators. GelMA has the cell adhesion and migration ability due to the presence of Arg-Gly-Asp (RGD) binding sequences and matrix metalloproteinase (MMP) degradable motifs in the polymer chains.⁸¹ However, long gelation time, poor mechanical and degradation properties of GelMA limit its applicability in 3D printing. To improve the shape fidelity of the printed

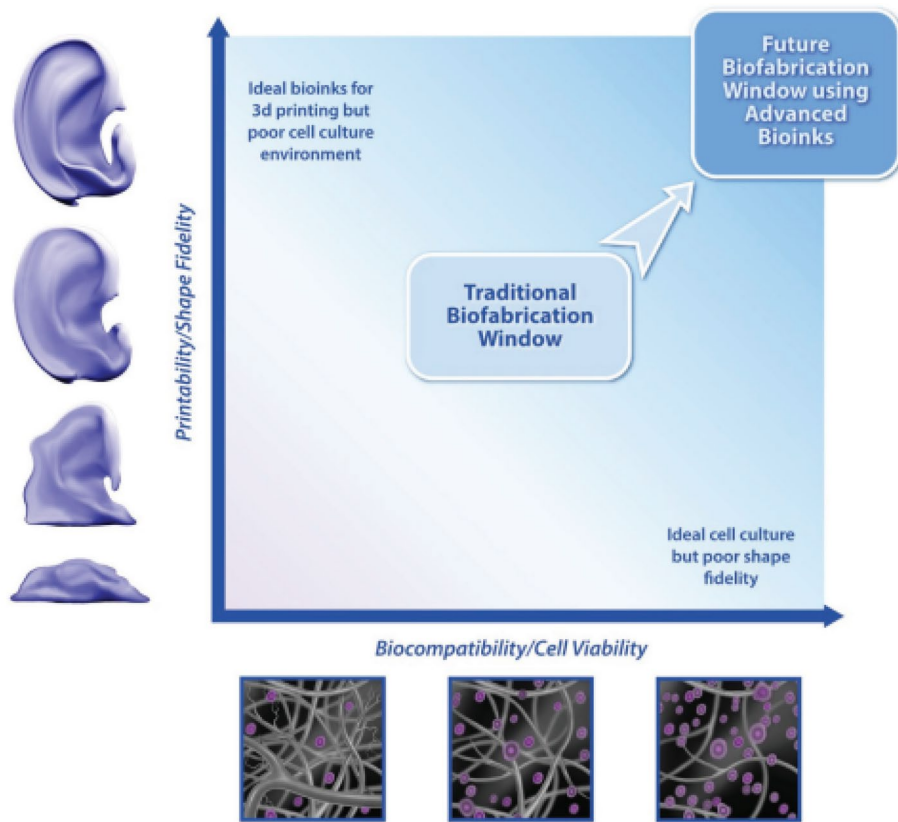


Figure 5: The biofabrication window describing the formulation of the traditional bioinks, which compromises the properties between structural fidelity and cell viability. High cell viability/excellent biocompatibility is obtained at low polymer concentration and/or crosslinking density of hydrogel networks, but a dense hydrogel network provides better shape fidelity. Advanced bioinks are the prospect for 3D bioprinting, where ideal bioinks are fabricated with tailored mechanical and biological properties.⁸⁰

construct, several biomaterials are blended with GelMA, and the composite bioinks are extensively used for tissue regeneration.

The components of multimaterial bioinks comprise several natural biopolymers, which are chemically crosslinked with non-identical synthetic or natural hydrogels in an appropriate proportion to optimize the bioprintability, biocompatibility and biodegradability. The natural biopolymers consist of several intrinsic cell-adhesion moieties, such as RGD moieties in collagen and gelatin, which act as the cell adhesion sites that lead to cell migration, proliferation and cell spreading. On the other hand, synthetic hydrogels consist of better mechanical properties, which enhances the structural integrity when combined with natural biopolymers. Polyethylene glycol (PEG) is a well-known nontoxic, non-immunogenic synthetic hydrogel, which exhibits excellent swelling and transport properties. These attributes can be blended with GelMA to develop

a photocrosslinkable, mechanically robust, cytocompatible and biodegradable composite hydrogel. Hutson et al. developed a PEG-GelMA based bioink with NIH3T3 fibroblasts.⁸² It was observed that the fibroblast spreading was enhanced within the composite hydrogel compared to single-component PEG. This study revealed that the compressive modulus and enzymatic degradation of the composite hydrogel could be tuned through the variation of the relative concentration of PEG and GelMA. In another study, Rutz et al. formulated a multimaterial bioink, where a multifunctional PEG crosslinker (PEGX) was blended with GelMA to improve the printability (Fig. 6).⁸³ Crosslinking density of the bioink depends on the functionality, concentration and molecular weight of PEGX. The functionality and chain length of PEGX were tailored to fabricate either soft or robust hydrogels. Viscosity and biodegradability of the printed construct can also be

Table 1: Summary of the use of gelatin methacrylate-based bioink in fabrication of different biological tissues/organs and drug screening.

Bioink composition	Cell type	Printing method	Bioink type	Printed construct	References
GelMA-PEGDMA	HUVECs	UV assisted capillary force lithography	Multimaterials	Nanopatterned vascular tissue	74
GelMA-PEG	NIH-3T3 fibroblast	Not performed	Multimaterial	–	82
GelMA-HAMA	HAVICs	Extrusion	Multimaterials	Heart valve	119
GelMA-HA-PCL	Human primary chondrocytes	Melt electrospinning in a direct writing mode	Multimaterial	Porous scaffold	120
GelMA-HyaMA	hADSCs	Not performed	Multimaterial	Composite scaffold	53
GelMA-collagen I	HUVECs, hMSCs	Microvalve-based drop-on-demand bioprinter	Multimaterial	Capillary-like network	52
GelMA-HA-PCL	Chondrocytes	Bio-scaffolder dispensing system	Multimaterial	Cartilage constructs	102
GelMA-HA-laminin-411	Human epithelial ovarian cancer cell line OV-MZ-6	Not studied	Multimaterials	3D cancer cell platform for ovarian cancer	121
GelMA-PEGDA	Mouse osteoblast	Not studied	Multimaterial	Bone tissue	122
GelMA-alginate	HUVECs, MDA-MB-231 and MCF7 breast cancer cells, NIH/3T3 mouse fibroblast	Coaxial extrusion nozzle setup	Multimaterials	Core/sheath micro-fibrous constructs	94
GelMA-PEGDA	MCF7, HUVECs, NIH/3T3 fibroblast, C2C12 skeletal muscle cells, mesenchymal stem cells (MSCs), fibroblasts, osteoblasts.	Microfluidic-stereolithography or multimaterial DMD (digital micromirror device) -based bioprinter	Multimaterials	Musculoskeletal systems,	99
GelMA-alginate	HUVECs	Microfluidic-based coaxial extrusion system	Multimaterials	Cardiac tissue	98
GelMA-alginate	HDFs, HepG2 (human hepatocellular cells), hMSCs, HUVECs	Multimaterial microfluidic bioprinting	Multimaterials	Human heart-like structure	97
GelMa-PEGX (X = multifunctional crosslinker)	human dermal fibroblasts (HDFs), HUVECs	ElvisionTEC 3D bioplotter	Multimaterial	Porous cylindrical scaffolds	83
GelMA- GGMA (gellan gum methacrylate)	NIH-3T3 fibroblasts	Not performed	Double network IPN	–	123
GelMA-SF (silk fibroin)	NIH-3T3 fibroblast	Combined photolithography and lyophilization	IPN	3D porous micro-scaffold	84
GelMA-collagen I	MDA-MB-231 breast tumour cell, endothelial cells (ECs)	Not performed	IPN	–	124
GelMA-CNT	NIH-3T3 fibroblast, human mesenchymal stem cells (hMSCs)	Not performed	Nanomaterials	–	86

Table 1: continued

Bioink composition	Cell type	Printing method	Bioink type	Printed construct	References
GelMA-GO (modified with acrylic functional groups)	NIH-3T3 fibroblasts	Sequential drop deposition and crosslinking	Nanomaterials	Multilayered cell-laden constructs	125
GelMA-chitosan NPs	NHDF	Not performed	Nanomaterials	–	87
GelMA-GNRs	Cardiomyocytes	Not performed	Nanomaterials	Cardiac tissue	126
GelMA-surface modified CNT	Neonatal rat cardiomyocytes	Not performed	Nanomaterials	Cardiac patches	127
GelMA-rGO (reduced graphin oxide: reduced with ascorbic acid)	Cardiomyocytes	Not performed	Nanomaterials	Myocardial tissue constructs	128
GelMA-Nanosilicates	MC3T3 preosteoblast	Extrusion	Nanomaterials	Scaffolds for bone tissue	85
GelMA-GG/PLA	Mesenchymal stromal cells (MSCs)	Extrusion based bioscaffold system	Microcarriers (PLA)	Bone tissue	92

optimized either by varying the PEGX functionality or degree of methacrylation.

Advanced bioinks can be fabricated using the interpenetrating network-based hydrogels (IPN). The term “interpenetrating network” is defined as the physical entanglement between multiple polymeric networks without forming any covalent bond (Fig. 7). In semi-IPNs, the polymeric networks have partial interaction and the individual polymeric network can be chemically crosslinked, but not crosslinked with other polymers. Xiao et al. developed a photocrosslinkable IPN-based bioink through the sequential polymerization of GelMA and silk fibroin (SF).⁸⁴ SF is the self-assembling structural protein, which has high mechanical strength, biocompatibility, oxygen transportation ability and ability to physical crosslink without chemical modification. During sequential printing, it was assumed that initially the exposed UV light photocrosslinked only the GelMA network without affecting the immobilized amorphous SF. This semi-IPN bioink was treated with aqueous methanol to crystallise the SF into β -sheet, which acts as the reinforcing component within GelMA matrix. It was illustrated that after methanol treatment on GelMA-SF semi-IPN, the compressive modulus enhanced significantly. It was also shown that the compressive modulus can be increased by fivefold when the SF concentration is increased from 0.5 to 2 wt%. The NIH-3T3 fibroblast cells were seeded on the hybrid hydrogel to study the cell behaviour. The GelMA-SF IPN bioink did not display significant cell spreading after 1 day in culture.

Though 0.5% SF concentration significantly increases the cell proliferation, however, incorporation of higher amount of SF reduces the proliferation rate of NIH-3T3 after 3 days of culture. This experiment suggested that optimal amount of SF with GelMA matrix can significantly increase the shape fidelity and biocompatibility.

Nanomaterials provide a high specific surface area, which promotes cell attachment, viability and proliferation. Besides, incorporation of nanomaterials can improve printability and mechanical strength and stiffness. Xavier et al. developed an osteoinductive GelMA-based bioink, where highly anisotropic nanosilicates were embedded for bone tissue regeneration (Fig. 8).⁸⁵ The shear thinning behaviour of the bioink was achieved through the non-covalent interaction of GelMA networks with the charged surface of nanosilicates. It was observed that the viscosity of the bioink, as well as the pore size of the printed construct, was increased with the addition of nanosilicate particles. The compressive modulus of 2% nanosilicate-incorporated GelMA solution was found to be enhanced by fourfold compared to GelMA hydrogel. The cell culture study revealed that nanosilicates did not significantly influence the initial cellular adhesion and metabolic activity up to 14 days of culture. Shin et al. investigated the mechanical properties and biocompatibility of carbon nano tube (CNT) reinforced GelMA bioink.⁸⁶ In this experiment, CNTs were coated with a thin layer of GelMA and next reinforced into the hydrogel matrix to enhance the biological properties. The encapsulated NIH-3T3 cells

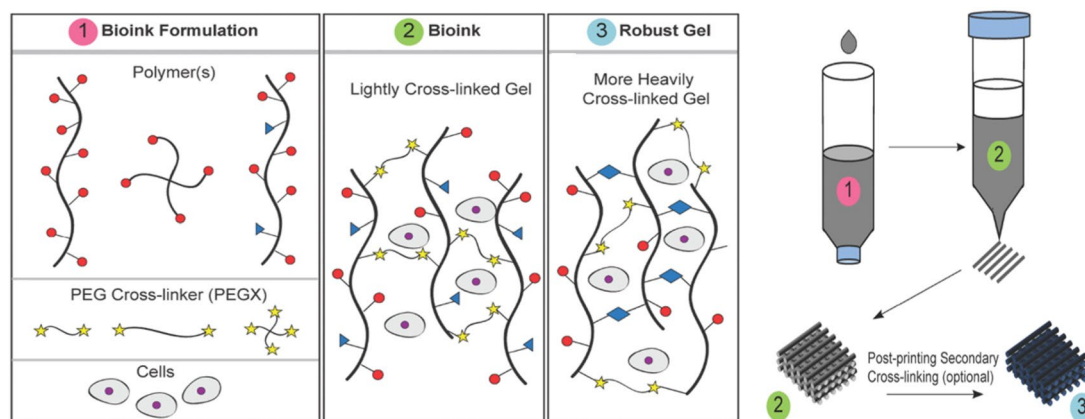


Figure 6: Schematic diagram of multimaterial bioink formulation using GelMA and PEG. The primary polymer molecules can be linear, branched or multifunctional (GelMA), whereas the chain length and functionality of PEGX crosslinker can be varied. During mixing, light crosslinking occurred through the coupling between the amine groups in GelMA and succinimidyl valerate groups in PEG. Robustness of the printed construct can be increased through UV light exposure⁴³

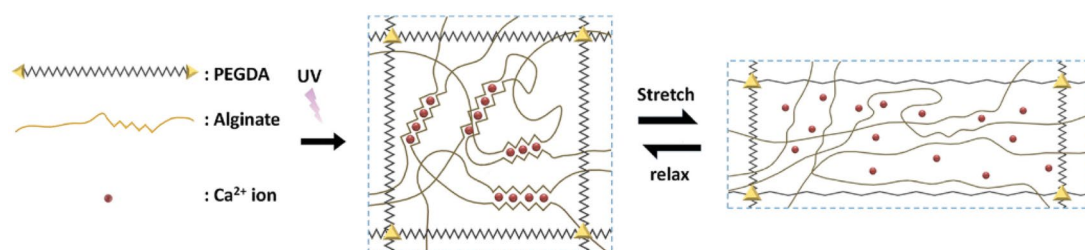


Figure 7: Fabrication of interpenetrating network (IPN) bioink from poly(ethylene glycol) and alginate hydrogels. The individual polymer chains of PEG and alginate were covalently crosslinked via UV exposure and ionically crosslinked using Ca^{2+} , respectively. The reversible physical crosslinking of alginate matrix and permanent bonding of PEG chains provide the shear thinning properties of IPN bioink¹¹⁷

showed high level of cellular viability and proliferation within the hybrid bioink during 48 h. In the cytotoxicity experiment, no significant cytotoxicity was observed up to a CNT concentration of 50 $\mu\text{g}/\text{ml}$. Furthermore, the GelMA-coated CNT-loaded bioink showed enhanced mechanical properties, specifically the elastic modulus, when compared to those of bare GelMA hydrogel. These results suggested that native tissue-like 3D structures can be fabricated by incorporating appropriate amount of CNTs into the GelMA matrix. Sometimes nanomaterials are loaded with hydrogels to release the growth factors in a controlled manner. Growth factors are the signalling molecules which are essential for promising tissue regeneration. Chitosan is a well-known biocompatible hydrogel, used for sustained release of growth factors. Modaresifar et al. developed a composite hydrogel made with GelMA and chitosan nanoparticles (NPs).⁸⁷ The chitosan NPs

were used as the nanocarrier that can deliver βFGF , an angiogenic growth factor within the hydrogel matrix. Normal human dermal fibroblasts (NHDF) were seeded and cultured within the composite hydrogel, and the effect of βFGF delivery on NHDF proliferation was investigated. It was shown that more than 75% of βFGF was released within 4 days, and after 7 days up to 90% was released. After 3 days of culture, the viability and proliferation of NHDF were significantly increased. GelMA/nanochitosan composite hydrogel showed higher swelling ratio (18.02 ± 0.4) compared to GelMA (15.04 ± 0.8), because of the presence of higher number of hydrophilic groups within the chitosan hydrogel network. This higher swelling ratio is an important factor, which influences the release and diffusion of growth factor to create a biomicro-environment. This result is expected to have a promising application for sustainable release of

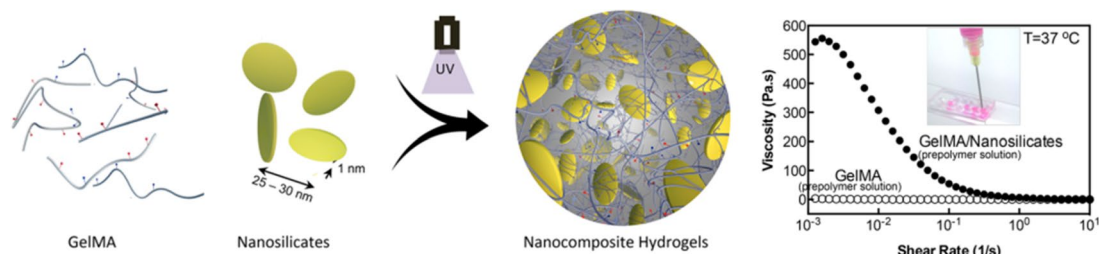


Figure 8: Bioactive ultrathin nanosilicate plates were loaded with GelMA hydrogel to fabricate nanomaterial-based bioink. The composite bioink shows shear thinning properties due to the incorporation of nanosilicates⁸⁵

growth factors within the 3D printed cell-laden microenvironment.

Supramolecular bioinks are the most recently developed advanced bioink, where various functional groups of short repeating units are physically interacted via hydrogen bonding, metal coordination, π - π stacking, crystalline domains and guest–host interaction to generate large polymeric entanglements. The non-covalent interaction between the several components provides a special arrangement of the hydrogel system. Due to the physical interaction, the bond between repeating units can be reversibly changed under shear stress during bioprinting. Therefore, the supramolecular bioinks can behave like a shear-thinning hydrogel. Under shear stress, viscosity of the bioinks reduces through the disruption of supramolecular bonds and the printing fidelity can be obtained through bond reconstruction. The known 3D printable biopolymers can be chemically modified and functionalized to tailor the supramolecular bonding, according to the desired mechanical and biological properties.⁸⁸ Highley et al. developed shear thinning supramolecular-based bioink, where the intermolecular bonds were formed through guest–host interaction.⁸⁹ In this experiment, hyaluronic acid (HA) was chemically modified with adamantane (Ad) and β -cyclodextrin (β -CD), and upon mixing Ad–HA and CD–HA, the supramolecular assemblies were formed via guest–host interaction between Ad and β -CD moieties. The bioink was printed within a support material and it was observed that after printing, the structure retains its desired shape over several days. Mesenchymal stem cells (MSCs) and 3T3 fibroblasts were encapsulated and printed to examine the toxicity of the bioink. Higher than 90% cell viability after 3 days of culture is a signature of the nontoxicity of the supramolecular bioink. Recently, Li et al. developed a supramolecular-based bioink, where the double network

was formed using poly(*N*-acryloyl glycinamide) (PNAGA) and Fe^{3+} coordinated carboxymethyl cellulose (CMC).⁹⁰ The supramolecular-based double network bioink consisted of two types of physical bonding. The first network was formed via metal coordination bonding of Fe^{3+} with the carboxyl groups of CMC and the second network was formed through dual amide hydrogen bonds of PNAGA (Fig. 9). The bioink showed excellent ability to recover the original shape after removal of mechanical forces that indicated the reversible physical crosslinking of supramolecular networks. Mechanical properties of the bioink were optimized via changing the concentration ratios of CMC and PNAGA. Mouse embryo fibroblast (L929) was seeded on the PNAGA/CMC- Fe bioink to determine cytotoxicity. The cellular viability was found to be more than 90% which confirmed that the supramolecular bioink was cytocompatible.

Besides nanomaterials, different microcarriers are incorporated with hydrogels to improve the hydrogel properties. Microcarriers are the porous biocompatible small bioactive particles, suspended into a hydrogel matrix for scalable bioprinting, initial seeding and expensive expansion of the cells. Sometimes microcarriers are blended to obtain the desired shape of the cells during differentiation and to guide them towards the desired cell fate. Microcarriers improve not only the printability of bioink, but also provide structural and mechanical support during tissue formation. Occasionally, microcarriers are added to the hydrogels in a higher amount until they do not clog in the printing nozzle in extrusion and inkjet bioprinting.⁹¹ Levato et al. developed a GelMA-gellan gum (GelMA-GG) based composite bioink in which polylactic acid was incorporated as the microcarriers.⁹² The printability and mechanical properties of microcarriers (MCs) loaded GelMA-GG were tested. The optimal concentration of MCs in GelMA-GG bioink was

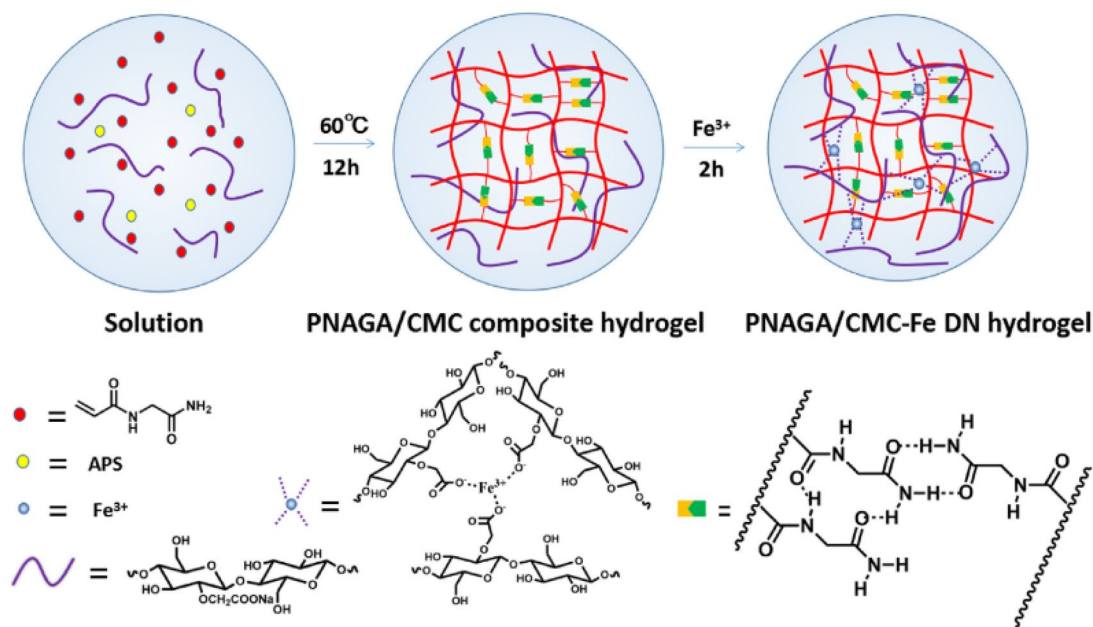


Figure 9: Proposed mechanism for supramolecular bioink synthesized using poly(*N*-acryloyl glycinamide) (PNAGA) and carboxymethyl cellulose (CMC). Fe^{3+} physically crosslinked CMC molecule via carboxyl-metal coordination bonding and PNAGA molecules are non-covalently crosslinked via dual amide hydrogen bonds ¹⁰

found to be 40 mg/ml without nozzle clogging through a 20-G conical nozzle in an extrusion-based bioprinter, while the printing speed was maintained at 475 mm/min at room temperature. From the mechanical properties point of view, it was seen that the compression modulus of the bioink was gradually increased with the increase of MCs' concentration. Mesenchymal stromal cells (MSCs) were embedded within the hybrid bioink and cultured for 21 days to investigate cell differentiation for bone regeneration. It was observed that after 3 days of bioprinting, more than 90% cells were viable. In the osteogenic culture media, the ALP activity and OCN secretion were increased over time, which indicated the suitability of poly(lactic acid) as MCs for osteogenic differentiation.

6 Advanced Bioprinting Techniques

Not only suitable biomaterials, appropriate bioprinting techniques are also required to fabricate complex tissue structure. The most straightforward method to build a biological tissue using multi-components is to fix a mixing device onto the printhead and extrude the bioink. However, the precise positioning of various bioinks as well as different cells cannot be possible using this method. Advanced bioprinting technologies should have the ability to print multiple

biomaterials, extracellular matrix and different types of cells to construct native tissues or organs with high resolution in a continuous and systematic manner. Sometimes, multiple print heads are loaded with 3D bioprinters to construct heterogeneous tissues or organ structures with several bioinks or different cell types (Fig. 10a). Before bioprinting, the cells are premixed with their respective bioink within the different print head and can be printed sequentially in a layer-by-layer manner. The major drawback of multi-head bioprinter is that only a single print head can be used at a time, which affects the alignments of the nozzles, start and off of the flow for a single layer of printing and resolution of the printed construct.⁹³ The other approach to print multicomponent bioink is coaxial 3D bioprinting.^{94, 95} In coaxial extrusion bioprinting, two different types of hydrogels are printed in a core/shell (*c/s*) fashion (Fig. 10b). Therefore, one hydrogel is printed as the core, which is radially encapsulated within the shell hydrogel. This printing method is used to modulate the mechanical properties and structural integrity of the printed construct.⁹⁶ Multi-material bioinks can also be printed using the multimaterial microfluidic bioprinting process.⁹⁷ In this technique, multiple bioinks can be integrated through the different microfluidic channel within the syringe barrel and dispensed through a single printhead as a fibre or droplet⁹⁸ (Fig. 10c).

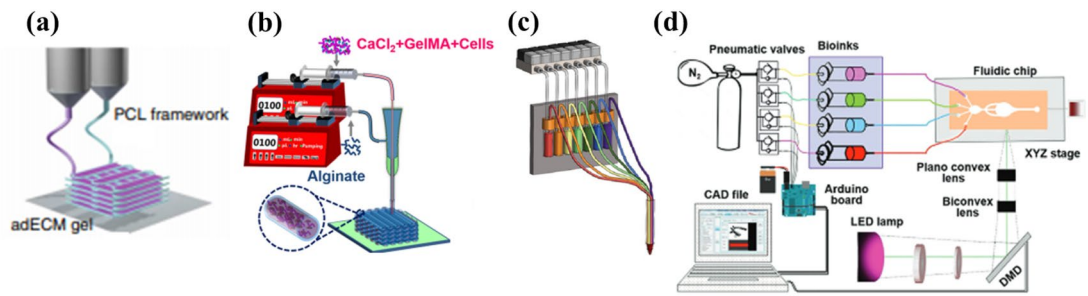


Figure 10: Schematic representation of different advanced bioprinting technologies such as **a** multihead bioprinting method, where decellularised extracellular matrix of adipose tissue (adECM) and polycaprolactone framework are used as multimaterial hydrogels,¹¹⁵ **b** coaxial bioprinting of GelMA (core) and alginate (shell),⁹⁴ **c** microfluidic bioprinting involves seven microfluidic channels which are connected to a single printhead,⁹⁷ **d** microfluidic stereolithography set up with the UV lamp, optical lenses, microfluidic device and DMD chip.⁹⁹

The microfluidic channels are selectively chosen to dispense specific hydrogels and cells in a programmable manner. This technique consists of fast switching between different microfluidic channels and simultaneous deposition of several hydrogels through a single nozzle. The individual microfluidic channels are connected with the pneumatic valves, which controls the pneumatic pressure to the bioinks that decide the viscosity and amount of individual bioinks to be printed. Another type of multimaterial 3D bioprinting approach is microfluidic stereolithography or multimaterial DMD (digital micromirror device), in which multiple hydrogels can be printed using a multi-inlet microfluidic chip⁹⁹ (Fig. 10d). This technology involves a microfluidic device which dynamically photopatterns different hydrogels on a moving stage. Hydrogels are sequentially injected into the microfluidic chip using the microfluidic device and are photo-crosslinked in a layer-by-layer fashion on the moving stage. The DMD technique comprises millions of microscopic mirrors to control the intensity of individual pixel, which can independently scan the bioink surface so that the special resolution of printing can be much higher compared to that of conventional STL technique.

7 Hydrogel-Based Bioprinted Tissues and Organs

It is very difficult to develop vascularized native functional tissues or organs with clinically relevant dimensions, because their complex structure consists of various cell types and biomolecules which are located in a precisely specified manner within the extracellular matrix. In the previous sections we have discussed various procedures

to invent advanced bioinks and some of the advanced bioprinting techniques which can be used to fabricate functional tissues that can replace damaged or failed native organs. Several attempts have been taken by different research groups to develop complete functional organs including blood vessels, cardiac valves, skin, bone and cartilage, liver, eye, ear, cardiac tissue and adipose tissue. In this review, we have discussed some specific 3D bioprinted functional organs such as ear, cartilage, brain and the urinary system, which provides the pathway of next generation tissue fabrication.

7.1 3D Bioprinted Cardiac Tissue

The heart is a very complex functional organ, which consists of several cell types such as cardiomyocytes, endothelial cells, fibroblasts, pacemaker cells and smooth muscle cells. To fabricate this structurally and functionally complex system with various cell types, multiple bioinks and advanced 3D bioprinting technologies are needed. Gaebel et al. fabricated a cardiac patch, embedded with HUVECs and hMSCs within polyester urethane urea (PEUU) bioink via laser-induced-forward-transfer (LIFT) bioprinting technology.¹⁰⁰ The fabricated patches consist of 91% porosity with 91 μm average pore size and 0.78 MPa tensile strength, and these were transplanted to the infarcted part of a rat heart. It was observed that there was a significant enhancement of angiogenesis on the border zone of the patch after 8 weeks of transplantation. The heart functionality and implant integrity were improved due to the vascular connection between native and implanted patch tissues. Gaetani et al. developed a multimaterial bioink consisting of gelatin and hyaluronic

acid to investigate the therapeutic potential of bioprinted cardiac patch that was implanted in a mouse heart.¹⁰¹ Human cardiac-derived progenitor cells (hCMPCs) were encapsulated within gel-HA bioink and a cardiogenic scaffold was bioprinted with 4 cm² surface area and 400 μm thickness. The *in vivo* experiment demonstrated the viability, proliferation, cardiac and vascular differentiation and preserved heart function of hCMPCs within the construct during 4 weeks of follow-up period. The optimal integration of the engrafted patch along the ventricular wall proved the potential for clinical transplantation.

7.2 3D Bioprinted Cartilage

Cartilage is a tough elastic connective tissue with the lack of vascularity, made up of chondrocyte cells surrounded by the glycoprotein materials, which is strengthened by collagen fibres. The major usage of cartilage tissue engineering is in plastic surgery, and the challenges of patient-specific cartilage regeneration are the optimization of mechanical properties like stiffness of tissues, which differ from the superficial sides to the interior. In addition, the pore size distribution within the bioprinted construct is an important factor for chondrocyte proliferation and cartilage regeneration. Malda and co-workers developed a GelMA/HA-based composite hydrogel, which was bioprinted through encapsulating chondrocytes to reconstruct articular cartilaginous tissues.¹⁰² Hydrogel viscosity, printability and swelling properties were optimized by varying the degree of gelatin methacrylation (40–75 ± 9%), concentration of hydrogel (5–20% GelMA) and UV dose (5–30 min exposure time). Enhanced mechanical properties were obtained through reinforcing thermoplastic PCL within the bioink consisting of 10% GelMA and 2.4% HA. After 3 days of cell culture, it was observed that the cell viability significantly increased and after 4 weeks, the presence of glycosaminoglycan indicated the formation of cartilage tissue. It was also reported that although HA enhances the viscosity and mechanical strength of hydrogels, it has no significant effect on chondrogenesis at a higher concentration. Apélgren et al. manufactured a 3D bioprinted scaffold using alginate and nanofibrillated cellulose-based bioink within which human bone marrow derived-MSCs (hBM-MSCs) and human nasal chondrocytes (hNCs) were encapsulated to fabricate cartilage tissue.¹⁰³ After extrusion, the construct (5 × 5 × 1.2-mm grid) was immediately transplanted into the subcutaneous pocket on the back of 48 8-week-old female

nude Balb/C mice. The morphological and immunohistochemical experiments on explanted tissues showed that after 30 days of implantation, 3.0 ± 5.7% surface area was covered by glycosaminoglycan (GAG)-positive hNCs, which was significantly increased to 17.2 ± 7.7% after 60 days. The cluster formation by GAG-positive chondrocytes and production of collagen type 2 within the ECM indicated that chondrocyte proliferation and cartilage regeneration occurred, *in vivo*. In another study, articular cartilage was developed using endogenic bone marrow stem cells (BMSCs) embedded silk fibroin and gelatin (SFG)-based bioink for the knee osteoarthritis tissue repair.¹⁰⁴ Gelatin and SF were premixed in an appropriate proportion (mass ratio of 1:2) to obtain optimum mechanical, biochemical and degradation properties of printed scaffolds. The pore size of the scaffold was maintained at 350 μm for appropriate chondrogenic differentiation. After chondrogenic induction with the SFG scaffold, round-shaped chondrogenic morphology was observed due to BMSC differentiation. Furthermore, the experiment revealed that with the incorporation of BMSC-specific-affinity peptide (E7) within SFG bioink, the GAG and collagen production was significantly enhanced, which indicated higher chondrogenic differentiation within SFG-E7 compared to that of SFG.

7.3 3D Bioprinted Bionic Ear

Mannoor et al. fabricated a bionic human ear made with cartilage tissue, which was intertwined with a silver nanoparticle (AgNPs) embedded conducting polymer and nonconducting silicone.¹⁰⁵ This experiment integrated functional biological tissues with nanoelectronic device through 3D printing. The geometry consisted of a cochlea-shaped electrode that transferred radiofrequencies (RF) to the inductive coil antenna, which was coupled with the ear auricle. The bioelectronics hybrid ear was printed through an extrusion-based Fab@Home 3D bioprinter. The auricle structure was constructed using an alginate hydrogel matrix in which chondrocyte cells were preseeded at a density of ~60 × 10⁶ cells/ml and 91.3 ± 3.9% cells were found to be viable after printing. During 10 weeks of chondrocyte culture, it was seen that the printed construct retain the shape fidelity and excellent cell viability. The results showed that the bioprinted ear has the capability to recognize the electromagnetic wave in RF range and they proposed that stereo audio music can be detected by the complementary right and left ears. Pati et al. constructed a

hybrid ear like scaffold structure, using polycaprolactone (PCL) and polyethylene glycol (PEG) as the framework and sacrificial layer, respectively, to provide the structural and mechanical support.¹⁰⁶ Three different types of hydrogels such as alginate (6%), atelocollagen (3%) and dECM were used to encapsulate human adipose derived stem cells (hASCs) and human turbinate tissue derived mesenchymal stem cells (hTMSCs) to infuse within the prefabricated PCL/PEG supporting network. A multi-head tissue/organ building system (MtoBS) was used to print the hydrogel encapsulated cells with the concentration of 10^6 cells/ml. After complete fabrication, the support layer was dissolved and removed using aqueous solutions without affecting cell viability and proliferation. The experiment showed the cell viability of $>95\%$ within all three types of hydrogel. In a similar study, Lee et al. fabricated 3D bioprinted ear-shaped structures using MtoBS bioprinter, where the cartilage (auricular) and fat (earlobe) tissues were developed by seeding with chondrocytes and adipocytes, respectively.¹⁰⁷ In this study, within the PCL/PEG support layer, cells embedded alginate hydrogel matrix was infused to provide the environment for chondrogenesis and adipogenesis during tissue regeneration. It was confirmed that adipose derived stromal cells (ASCs) differentiated into chondrocytes and adipocytes into the hydrogel matrix within a week and the cellular viability was found to be 95%. Kang et al. fabricated human ear like tissue construct using an integrated tissue-organ printer (ITOP).¹⁰⁸ Biodegradable supporting polymers (PCL) and sacrificial hydrogels (Pluronic F-127) were simultaneously extruded with the cell-laden hydrogel to impart mechanical support. In addition, during printing microchannels were created through PCL patterns within the hydrogel matrix for proper nutrient and oxygen diffusion within the tissue construct. The cells were encapsulated within a multimaterial-based composite hydrogel consisting of gelatin, fibrinogen, glycerol and hyaluronic acid. Before final printing, the concentration of each hydrogel and cell density was optimized to achieve the best printing resolution, shape fidelity and cell viability. To fabricate the human size auricle construct, the rabbit ear chondrocytes were encapsulated with the density of 40×10^6 cells/ml, where the concentrations of gelatin, fibrinogen, HA and glycerol were optimized at 45 mg/ml, 30 mg/ml, 3 mg/ml, and 10% v/v, respectively. After 1 day of culture, the cellular viability was found to be $91 \pm 8\%$ and after 5 weeks of culture, formation of new viable cartilage construct was found with

similar morphological characteristics of native tissue. Markstedt et al. developed a bioprinted human ear, where human nasoseptal chondrocytes (hNC) were embedded within a nanomaterials-based bioink developed with nanofibrillated cellulose (NFC) and alginate.¹⁰⁹ To improve the bioink viscosity, printing resolution, and shape fidelity of the printed construct, NFC was used intentionally as the primary bioink. 90% NFC and 10% alginate (INK9010) were used to investigate cytotoxicity of NFC and on chondrocyte cells no potential cytotoxicity was found. The respective cells viability was found to be $72.8 \pm 6\%$ and $85.7 \pm 1.9\%$, after 1 and 7 days of cell culture within Ink8020 construct.

7.4 3D Bioprinted Brain Like Tissue

Brain is the most complex functional organ compared to any other tissue and organ. Therefore, fabrication of the complete structural brain with several cell types using 3D printing is far from success. A few attempts have been taken by different research groups. Lozano et al. manufactured a 3D brain like structure, where the primary cortical neural cells were encapsulated within a peptide modified gellan gum (RGD-GG)-based bioink.¹¹⁰ The cells, concentration was optimized at 1×10^6 cells/ml within the 0.5% (w/v) RGD-GG bioink solution and was bioprinted using their own developed handheld bioprinter. It was confirmed that the peptide (RGD) modification of GG improved the cell hydrogel interaction, which highly influenced cell survival, proliferation, differentiation and neuron network formation. This experiment also revealed that the survival, spreading and differentiation of glial cells within the RGD-GG matrix. The bioprinted construct showed sufficient shape fidelity with the pore diameter distribution ranging from 10 to 250 μm , which facilitate for oxygen, nutrient and cell metabolic waste transportation during cell culture. After 5 days of neural cell culture within printed RGD-GG, $73 \pm 8\%$ cells were found to be viable. In an extended study, cortical neurons were embedded within a 1% (w/v) RGD-GG matrix and cultured in Neurobasal media for cell maturation for 7 day.¹¹¹ The bioprinted cells were immunostained with different antibodies. The confocal images demonstrated a homogeneous distribution of cortical neurons, which formed a highly interconnected neuronal network throughout the RGD-GG matrix. This study proposed to develop multilayered brain model for in vitro neuronal cell study. Recently, Heinrich et al. developed a bioprinted miniaturized

brain model (4 mm × 6 mm × 5 mm) to understand the interaction mechanism and biological relevance between macrophages and glioblastoma cells towards glioblastoma-associated macrophages (GAMs) *in vitro*.¹¹² Tumour cells and macrophages were encapsulated within a GelMA (3% w/v) and gelatin (4% w/v) based composite bioink, which were extruded into the mini-brain shaped model and phenotypic alterations of both cancer cells and macrophages were investigated. The two step bioprinting process involved through the construction of an empty mini-brain cavity with mouse macrophages cell line (RAW264.7) within which the mouse glioblastoma cells (GL261) cells were printed. The multimaterial bioink displayed promising shear thinning properties and the printed construct showed excellent mechanical and structural stability with the storage modulus of 1 kPa and loss modulus of 10–20 Pa. The immunofluorescent staining and SEM for GL261 and RAW264.7 cells respectively confirmed the cellular adherence with the printed bioink matrix. The post-printing study showed high metabolic activity and cellular viability of both the cell lines up to 10 days. The crosstalk experiment between the macrophages and tumour cells showed the recapitulation of phenotype characteristics and enhanced gene expression compared to that of conventional 2D cell culture. It was revealed that the macrophages migrated towards the tumour cells and support them for significant growth and survival. Finally, this model demonstrated to create a realistic 3D environment to investigate glioblastoma metastasis, conventional chemotherapy and test drug delivery which provided the confidence for *in vivo* experiment.

7.5 3D Bioprinted Urinary System

The urinary system consists of the kidney, ureter, bladder and urethra. Since the kidney is a structurally and functionally complex organ in the urinary system, several attempts have been taken to reconstruct urological hollow organs, specifically of the lower urinary tract like bladder and urethra. The collagen-rich connective tissue in between muscle and epithelium tissues must be printed in a specific manner to fabricate urinary tissues, which should have the sufficient elasticity for functional contraction and relaxation. Zhang et al. developed circumferentially multilayered tubular tissue-like urethra using multichannel co-axial extrusion system (MCCES)-based bioprinter.¹¹³ Human urothelial cells (HUCs) and human bladder smooth muscle cells (HBdSMCs)

were suspended into a customized multimaterial bioink, consisting with GelMA, alginate and eight-arm poly(ethylene glycol) acrylate to construct the urothelial tissue. To improve the mechanical stability of the hollow tube, the crosslinking mechanism involved two steps. After ionically crosslinking of alginate with CaCl₂, the construct was exposed to UV light to photocrosslink the remaining hydrogel matrix components. After 7 days of culture, the cellular viability was found to be 89 ± 3%, indicating that the customized bioink was suitable for creation of microcellular environment for HUCs and HBdSMCs. In another study, Zhang et al. bioprinted spiral scaffold structure using poly(ε-caprolactone) and poly(lactic-co-caprolactone) (PCL/PLCL) synthetic polymers within which gelatin, fibrin, and hyaluronic acid based multimaterial bioink were incorporated to mimic the urethra.¹¹⁴ The bladder epithelial cells (UCs) and smooth muscle cells (SMCs) were loaded with cell-laden hydrogel to develop the respective inner and outer tissues of urethra. After 7 days of bioprinting, the cellular viability of both the cells was found to be higher than 80% with active proliferation and spreading. The cellular growth within the scaffold pores and cellular interaction between UCs and SMCs indicated the *in vivo* urethral implantation in animal models. Imamura et al. bioprinted a bladder-like structure using bone marrow derived cells, harvested from femurs of rat to repair radiation-injured rat urinary bladder.¹¹⁵ This technique involved scaffold-free 3D printing technology, where the spheroids were suspended (4.0 × 10⁴ cells/0.1 ml of cell suspension media) and deposited onto microneedle array. The cell spheroids were assembled into three layers with the height of 1 mm. After the removal of microneedle arrays (7 days), the spheroids were self-assembled and started to proliferate with the secretion of ECM. The fabricated structure was transplanted in the anterior wall of the radiation-injured rat bladder. It was observed that the transplanted structure readily recognized the transplanted region and survived through the nerve reconstruction, and blood vessels were grown through the transplanted structure from the native bladder after 4 weeks of surgery. This indicated that the transplanted biofabricated structure successfully restores the functionality of injured bladder.

8 Closure

3D bioprinting affords high-throughput capability to develop 3D viable tissue construct, which can serve as the functional native tissue with similar

cell types and density. Hydrogel-based biomaterials become the most promising candidate for cell carrier and construct fabrication in 3D bioprinting. The hydrogel matrix provides temporarily an extracellular matrix-like environment towards the printed cells, such that they can survive, proliferate and differentiate to regenerate a desired tissue or organ. Not only the biological microenvironment but also the mechanical and structural integrity are provided, such that shape fidelity of the construct is maintained during the tissue reconstruction. Besides the structural and biological properties, the hydrogels should have proper rheological properties, gelation, transportation and degradation mechanisms. Since native tissues are composed of very complex structures, within which different cells are precisely located to preserve the tissue functionality, advanced bioinks and bioprinting technologies are adapted to replicate native tissues and organs. Moreover, the bioprinted constructs can provide the native tissue-like environment within which in vitro drug delivery and clinical studies can be performed. As a future vision, 3D bioprinting offers a new strategy which can replace conventional tissue engineering, cancer therapy and drug delivery experiments.

Publisher's Note

Springer Nature remains neutral with regard to jurisdictional claims in published maps and institutional affiliations.

Received: 12 September 2019 Accepted: 23 September 2019
Published online: 9 October 2019

References

- Mironov V et al (2009) Biofabrication: a 21st century manufacturing paradigm. *Biofabrication* 1(2):022001
- Liu C, Xia Z, Czernuszka J (2007) Design and development of three-dimensional scaffolds for tissue engineering. *Chem Eng Res Des* 85(7):1051–1064
- Chan B, Leong K (2008) Scaffolding in tissue engineering: general approaches and tissue-specific considerations. *Eur Spine J* 17(4):467–479
- Bajaj P et al (2014) 3D biofabrication strategies for tissue engineering and regenerative medicine. *Annu Rev Biomed Eng* 16:247–276
- Fong ELS et al (2013) Modeling Ewing sarcoma tumors in vitro with 3D scaffolds. *Proc Natl Acad Sci* 110(16):6500–6505
- Lee MK et al (2015) A bio-inspired, microchanneled hydrogel with controlled spacing of cell adhesion ligands regulates 3D spatial organization of cells and tissue. *Biomaterials* 58:26–34
- Murphy SV, Atala A (2014) 3D bioprinting of tissues and organs. *Nat Biotechnol* 32(8):773
- Ozolat IT, Yu Y (2013) Bioprinting toward organ fabrication: challenges and future trends. *IEEE Trans Biomed Eng* 60(3):691–699
- Malda J et al (2013) 25th anniversary article: engineering hydrogels for biofabrication. *Adv Mater* 25(36):5011–5028
- Melchels FP et al (2012) Additive manufacturing of tissues and organs. *Prog Polym Sci* 37(8):1079–1104
- Norotte C et al (2009) Scaffold-free vascular tissue engineering using bioprinting. *Biomaterials* 30(30):5910–5917
- Jakab K et al (2010) Tissue engineering by self-assembly and bio-printing of living cells. *Biofabrication* 2(2):022001
- Yu Y et al (2016) Three-dimensional bioprinting using self-assembling scalable scaffold-free “tissue strands” as a new bioink. *Sci Rep* 6:28714
- Pourchet LJ et al (2017) Human skin 3D bioprinting using scaffold-free approach. *Adv Healthc Mater* 6(4):1601101
- Yu Y, Ozolat IT (2014) Tissue strands as “bioink” for scale-up organ printing. in 2014 36th Annual International Conference of the IEEE Engineering in Medicine and Biology Society, 2014, IEEE
- Wu Z et al (2016) Bioprinting three-dimensional cell-laden tissue constructs with controllable degradation. *Sci Rep* 6:24474
- Chua CK, Yeong WY (2014) *Bioprinting: principles and applications*, vol 1. World Scientific, Singapore
- Schuurman W et al (2011) Bioprinting of hybrid tissue constructs with tailorable mechanical properties. *Biofabrication* 3(2):021001
- Chimene D et al (2016) Advanced bioinks for 3D printing: a materials science perspective. *Ann Biomed Eng* 44(6):2090–2102
- Derby B (2012) Printing and prototyping of tissues and scaffolds. *Science* 338(6109):921–926
- Chia HN, Wu BM (2015) Recent advances in 3D printing of biomaterials. *J Biol Eng* 9(1):4
- Kumar A et al (2016) Low temperature additive manufacturing of three dimensional scaffolds for bone-tissue engineering applications: processing related challenges and property assessment. *Mater Sci Eng* 103:1–39
- Panwar A, Tan L (2016) Current status of bioinks for micro-extrusion-based 3D bioprinting. *Molecules* 21(6):685
- Ozolat IT, Hospodiuk M (2016) Current advances and future perspectives in extrusion-based bioprinting. *Biomaterials* 76:321–343
- Arai K et al (2011) Three-dimensional inkjet biofabrication based on designed images. *Biofabrication* 3(3):034113
- Cui X et al (2012) Thermal inkjet printing in tissue engineering and regenerative medicine. *Recent Pat Drug Deliv Formul* 6(2):149–155

27. Guillemot F et al (2010) Laser-assisted cell printing: principle, physical parameters versus cell fate and perspectives in tissue engineering. *Nanomedicine* 5(3):507–515
28. Hribar KC et al (2014) Light-assisted direct-write of 3D functional biomaterials. *Lab Chip* 14(2):268–275
29. Aguado BA et al (2011) Improving viability of stem cells during syringe needle flow through the design of hydrogel cell carriers. *Tissue Eng Part A* 18(7–8):806–815
30. Chang R, Nam J, Sun W (2008) Effects of dispensing pressure and nozzle diameter on cell survival from solid freeform fabrication-based direct cell writing. *Tissue Eng Part A* 14(1):41–48
31. Kang K, Hockaday L, Butcher J (2013) Quantitative optimization of solid freeform deposition of aqueous hydrogels. *Biofabrication* 5(3):035001
32. Cui X et al (2010) Cell damage evaluation of thermal inkjet printed Chinese hamster ovary cells. *Biotechnol Bioeng* 106(6):963–969
33. Gurkan UA et al (2014) Engineering anisotropic biomimetic fibrocartilage microenvironment by bioprinting mesenchymal stem cells in nanoliter gel droplets. *Mol Pharm* 11(7):2151–2159
34. Gudapati H, Dey M, Ozbolat I (2016) A comprehensive review on droplet-based bioprinting: past, present and future. *Biomaterials* 102:20–42
35. Ferris CJ et al (2013) Bio-ink for on-demand printing of living cells. *Biomater Sci* 1(2):224–230
36. Arslan-Yildiz A et al (2016) Towards artificial tissue models: past, present, and future of 3D bioprinting. *Biofabrication* 8(1):014103
37. Guillotin B, Guillemot F (2011) Cell patterning technologies for organotypic tissue fabrication. *Trends Biotechnol* 29(4):183–190
38. Koch L et al (2012) Skin tissue generation by laser cell printing. *Biotechnol Bioeng* 109(7):1855–1863
39. Skardal A, Atala A (2015) Biomaterials for integration with 3-D bioprinting. *Ann Biomed Eng* 43(3):730–746
40. Schiele NR et al (2010) Laser-based direct-write techniques for cell printing. *Biofabrication* 2(3):032001
41. Ahmed EM (2015) Hydrogel: preparation, characterization, and applications: a review. *J Adv Res* 6(2):105–121
42. Seliktar D (2012) Designing cell-compatible hydrogels for biomedical applications. *Science* 336(6085):1124–1128
43. Gungor-Ozkerim PS et al (2018) Bioinks for 3D bioprinting: an overview. *Biomater Sci* 6(5):915–946
44. Gasperini L, Mano JF, Reis RL (2014) Natural polymers for the microencapsulation of cells. *J R Soc Interface* 11(100):20140817
45. Tan H, Marra KG (2010) Injectable, biodegradable hydrogels for tissue engineering applications. *Materials* 3(3):1746–1767
46. Hennink WE, van Nostrum CF (2012) Novel crosslinking methods to design hydrogels. *Adv Drug Deliv Rev* 64:223–236
47. Jungst T et al (2015) Strategies and molecular design criteria for 3D printable hydrogels. *Chem Rev* 116(3):1496–1539
48. Chenite A et al (2000) Novel injectable neutral solutions of chitosan form biodegradable gels in situ. *Biomaterials* 21(21):2155–2161
49. Ikada Y et al (1987) Stereocomplex formation between enantiomeric poly (lactides). *Macromolecules* 20(4):904–906
50. Lim DW, Park TG (2000) Stereocomplex formation between enantiomeric PLA-PEG-PLA triblock copolymers: characterization and use as protein-delivery microparticulate carriers. *J Appl Polym Sci* 75(13):1615–1623
51. Na K et al (2018) Effect of solution viscosity on retardation of cell sedimentation in DLP 3D printing of gelatin methacrylate/silk fibroin bioink. *J Ind Eng Chem* 61:340–347
52. Strateffien H et al (2017) GelMA-collagen blends enable drop-on-demand 3D printability and promote angiogenesis. *Biofabrication* 9(4):045002
53. Kessler L et al (2017) Methacrylated gelatin/hyaluronan-based hydrogels for soft tissue engineering. *J Tissue Eng* 8:2041731417744157
54. Billiet T et al (2014) The 3D printing of gelatin methacrylamide cell-laden tissue-engineered constructs with high cell viability. *Biomaterials* 35(1):49–62
55. Pawar AA et al (2016) High-performance 3D printing of hydrogels by water-dispersible photoinitiator nanoparticles. *Sci Adv* 2(4):e1501381
56. Fairbanks BD et al (2009) Photoinitiated polymerization of PEG-diacrylate with lithium phenyl-2, 4, 6-trimethylbenzoylphosphinate: polymerization rate and cytocompatibility. *Biomaterials* 30(35):6702–6707
57. Martinez PR et al (2017) Fabrication of drug-loaded hydrogels with stereolithographic 3D printing. *Int J Pharm* 532(1):313–317
58. Wang Z, et al. (2017) Visible light-based stereolithography bioprinting of cell-adhesive gelatin hydrogels in 2017 39th Annual International Conference of the IEEE Engineering in Medicine and Biology Society (EMBC), 2017, IEEE
59. Wang Z et al (2015) A simple and high-resolution stereolithography-based 3D bioprinting system using visible light crosslinkable bioinks. *Biofabrication* 7(4):045009
60. Ehsan SM et al (2014) A three-dimensional in vitro model of tumor cell intravasation. *Integr Biol* 6(6):603–610
61. Sperinde JJ, Griffith LG (1997) Synthesis and characterization of enzymatically-cross-linked poly (ethylene glycol) hydrogels. *Macromolecules* 30(18):5255–5264
62. Yang C et al (2015) Hyaluronic acid nanogels with enzyme-sensitive cross-linking group for drug delivery. *J Control Release* 205:206–217
63. Lee F, Chung JE, Kurisawa M (2008) An injectable enzymatically crosslinked hyaluronic acid-tyramine

- hydrogel system with independent tuning of mechanical strength and gelation rate. *Soft Matter* 4(4):880–887
64. Jin R et al (2010) Enzymatically-crosslinked injectable hydrogels based on biomimetic dextran–hyaluronic acid conjugates for cartilage tissue engineering. *Biomaterials* 31(11):3103–3113
 65. Raia NR et al (2017) Enzymatically crosslinked silk–hyaluronic acid hydrogels. *Biomaterials* 131:58–67
 66. Bakota EL et al (2010) Enzymatic cross-linking of a nanofibrous peptide hydrogel. *Biomacromolecules* 12(1):82–87
 67. Das S et al (2015) Bioprintable, cell-laden silk fibroin–gelatin hydrogel supporting multilineage differentiation of stem cells for fabrication of three-dimensional tissue constructs. *Acta Biomater* 11:233–246
 68. Bouhadir KH et al (2001) Degradation of partially oxidized alginate and its potential application for tissue engineering. *Biotechnol Prog* 17(5):945–950
 69. Jia J et al (2014) Engineering alginate as bioink for bioprinting. *Acta Biomater* 10(10):4323–4331
 70. Grigore A et al (2014) Behavior of encapsulated MG-63 cells in RGD and gelatine-modified alginate hydrogels. *Tissue Eng Part A* 20(15–16):2140–2150
 71. Schloßmacher U et al (2013) Alginate/silica composite hydrogel as a potential morphogenetically active scaffold for three-dimensional tissue engineering. *RSC Adv* 3(28):11185–11194
 72. Lee JM, Yeong WY (2016) Design and printing strategies in 3D bioprinting of cell-hydrogels: a review. *Adv Healthc Mater* 5(22):2856–2865
 73. Busilacchi A et al (2013) Chitosan stabilizes platelet growth factors and modulates stem cell differentiation toward tissue regeneration. *Carbohydr Polym* 98(1):665–676
 74. Kim P et al (2014) Fabrication of poly (ethylene glycol): gelatin methacrylate composite nanostructures with tunable stiffness and degradation for vascular tissue engineering. *Biofabrication* 6(2):024112
 75. Miri AK et al (2019) Effective bioprinting resolution in tissue model fabrication. *Lab Chip* 19(11):2019–2037
 76. Tirella A et al (2009) A phase diagram for microfabrication of geometrically controlled hydrogel scaffolds. *Biofabrication* 1(4):045002
 77. Pepelanova I et al (2018) Gelatin-methacryloyl (GelMA) hydrogels with defined degree of functionalization as a versatile toolkit for 3D cell culture and extrusion bioprinting. *Bioengineering* 5(3):55
 78. Kirschner CM, Anseth KS (2013) Hydrogels in healthcare: from static to dynamic material microenvironments. *Acta Mater* 61(3):931–944
 79. Ahearne M (2014) Introduction to cell–hydrogel mechanosensing. *Interface Focus* 4(2):20130038
 80. Kyle S et al (2017) Printability of candidate biomaterials for extrusion based 3D printing: state-of-the-art. *Adv Healthc Mater* 6(16):1700264
 81. Ramon-Azcon J et al (2012) Gelatin methacrylate as a promising hydrogel for 3D microscale organization and proliferation of dielectrophoretically patterned cells. *Lab Chip* 12(16):2959–2969
 82. Hutson CB et al (2011) Synthesis and characterization of tunable poly (ethylene glycol): gelatin methacrylate composite hydrogels. *Tissue Eng Part A* 17(13–14):1713–1723
 83. Rutz AL et al (2015) A multimaterial bioink method for 3D printing tunable, cell-compatible hydrogels. *Adv Mater* 27(9):1607–1614
 84. Xiao W et al (2011) Synthesis and characterization of photocrosslinkable gelatin and silk fibroin interpenetrating polymer network hydrogels. *Acta Biomater* 7(6):2384–2393
 85. Xavier JR et al (2015) Bioactive nanoengineered hydrogels for bone tissue engineering: a growth-factor-free approach. *ACS Nano* 9(3):3109–3118
 86. Shin SR et al (2011) Carbon nanotube reinforced hybrid microgels as scaffold materials for cell encapsulation. *ACS Nano* 6(1):362–372
 87. Modaresifar K, Hadjizadeh A, Niknejad H (2018) Design and fabrication of GelMA/chitosan nanoparticles composite hydrogel for angiogenic growth factor delivery. *Artif Cells Nanomedicine Biotechnol* 46(8):1799–1808
 88. Pekkanen AM et al (2017) 3D printing polymers with supramolecular functionality for biological applications. *Biomacromolecular* 18(9):2669–2687
 89. Highley CB, Rodell CB, Burdick JA (2015) Direct 3D printing of shear-thinning hydrogels into self-healing hydrogels. *Adv Mater* 27(34):5075–5079
 90. Li H et al (2018) A highly tough and stiff supramolecular polymer double network hydrogel. *Polymer* 153:193–200
 91. Hospodiuk M et al (2017) The bioink: a comprehensive review on bioprintable materials. *Biotechnol Adv* 35(2):217–239
 92. Levato R et al (2014) Biofabrication of tissue constructs by 3D bioprinting of cell-laden microcarriers. *Biofabrication* 6(3):035020
 93. Ashammakhi N et al (2019) Bioinks and bioprinting technologies to make heterogeneous and biomimetic tissue constructs. *Mater Today Bio* 1:100008
 94. Liu W et al (2018) Coaxial extrusion bioprinting of 3D microfibrillar constructs with cell-favorable gelatin methacryloyl microenvironments. *Biofabrication* 10(2):024102
 95. Gao Q et al (2015) Coaxial nozzle-assisted 3D bioprinting with built-in microchannels for nutrients delivery. *Biomaterials* 61:203–215
 96. Mistry P et al (2017) Bioprinting using mechanically robust core–shell cell-laden hydrogel strands. *Macromol Biosci* 17(6):1600472
 97. Liu W et al (2017) Rapid continuous multimaterial extrusion bioprinting. *Adv Mater* 29(3):1604630

98. Colosi C et al (2016) Microfluidic bioprinting of heterogeneous 3D tissue constructs using low-viscosity bioink. *Adv Mater* 28(4):677–684
99. Miri AK et al (2018) Microfluidics-enabled multimaterial maskless stereolithographic bioprinting. *Adv Mater* 30(27):1800242
100. Gaebel R et al (2011) Patterning human stem cells and endothelial cells with laser printing for cardiac regeneration. *Biomaterials* 32(35):9218–9230
101. Gaetani R et al (2015) Epicardial application of cardiac progenitor cells in a 3D-printed gelatin/hyaluronic acid patch preserves cardiac function after myocardial infarction. *Biomaterials* 61:339–348
102. Schuurman W et al (2013) Gelatin-methacrylamide hydrogels as potential biomaterials for fabrication of tissue-engineered cartilage constructs. *Macromol Biosci* 13(5):551–561
103. Apelgren P et al (2017) Chondrocytes and stem cells in 3D-bioprinted structures create human cartilage in vivo. *PLoS One* 12(12):e0189428
104. Shi W et al (2017) Structurally and functionally optimized silk-fibroin–gelatin scaffold using 3D printing to repair cartilage injury in vitro and in vivo. *Adv Mater* 29(29):1701089
105. Mannoor MS et al (2013) 3D printed bionic ears. *Nano Lett* 13(6):2634–2639
106. Pati F et al (2013) 3D printing of cell-laden constructs for heterogeneous tissue regeneration. *Manuf Lett* 1(1):49–53
107. Lee J-S et al (2014) 3D printing of composite tissue with complex shape applied to ear regeneration. *Biofabrication* 6(2):024103
108. Kang H-W et al (2016) A 3D bioprinting system to produce human-scale tissue constructs with structural integrity. *Nat Biotechnol* 34(3):312
109. Markstedt K et al (2015) 3D bioprinting human chondrocytes with nanocellulose–alginate bioink for cartilage tissue engineering applications. *Biomacromolecules* 16(5):1489–1496
110. Lozano R et al (2015) 3D printing of layered brain-like structures using peptide modified gellan gum substrates. *Biomaterials* 67:264–273
111. Lozano R et al (2016) Brain on a bench top. *Mater Today* 19(2):124–125
112. Heinrich MA et al (2019) 3D-bioprinted mini-brain: a glioblastoma model to study cellular interactions and therapeutics. *Adv Mater* 31(14):1806590
113. Pi Q et al (2018) Digitally tunable microfluidic bioprinting of multilayered cannular tissues. *Adv Mater* 30(43):1706913
114. Zhang K et al (2017) 3D bioprinting of urethra with PCL/PLCL blend and dual autologous cells in fibrin hydrogel: an in vitro evaluation of biomimetic mechanical property and cell growth environment. *Acta Biomater* 50:154–164
115. Imamura T et al (2018) Biofabricated structures reconstruct functional urinary bladders in radiation-injured rat bladders. *Tissue Eng Part A* 24(21–22):1574–1587
116. Gopinathan J, Noh I (2018) Recent trends in bioinks for 3D printing. *Biomater Res* 22(1):11
117. Hong S et al (2015) 3D printing of highly stretchable and tough hydrogels into complex, cellularized structures. *Adv Mater* 27(27):4035–4040
118. Pati F et al (2014) Printing three-dimensional tissue analogues with decellularized extracellular matrix bioink. *Nat Commun* 5:3935
119. Duan B et al (2014) Three-dimensional printed trileaflet valve conduits using biological hydrogels and human valve interstitial cells. *Acta Biomater* 10(5):1836–1846
120. Visser J et al (2015) Reinforcement of hydrogels using three-dimensionally printed microfibrils. *Nat Commun* 6:6933
121. Kaemmerer E et al (2014) Gelatine methacrylamide-based hydrogels: an alternative three-dimensional cancer cell culture system. *Acta Biomater* 10(6):2551–2562
122. Wang Y et al (2018) Development of a photo-crosslinking, biodegradable GelMA/PEGDA hydrogel for guided bone regeneration materials. *Materials* 11(8):1345
123. Shin H, Olsen BD, Khademhosseini A (2012) The mechanical properties and cytotoxicity of cell-laden double-network hydrogels based on photocrosslinkable gelatin and gellan gum biomacromolecules. *Biomaterials* 33(11):3143–3152
124. Berger AJ et al (2017) Decoupling the effects of stiffness and fiber density on cellular behaviors via an interpenetrating network of gelatin-methacrylate and collagen. *Biomaterials* 141:125–135
125. Shin SR et al (2013) Cell-laden microengineered and mechanically tunable hybrid hydrogels of gelatin and graphene oxide. *Adv Mater* 25(44):6385–6391
126. Navaei A et al (2016) Gold nanorod-incorporated gelatin-based conductive hydrogels for engineering cardiac tissue constructs. *Acta Biomater* 41:133–146
127. Shin SR et al (2013) Carbon-nanotube-embedded hydrogel sheets for engineering cardiac constructs and bioactuators. *ACS Nano* 7(3):2369–2380
128. Shin SR et al (2016) Reduced graphene oxide–gelMA hybrid hydrogels as scaffolds for cardiac tissue engineering. *Small* 12(27):3677–3689



Mr. Soumitra Das is a Ph.D. scholar in the group of Laboratory of biomaterials, Materials Research Centre at Indian Institute of Science, Bangalore (India). He received his B.Sc. in industrial chemistry (2014) and M.Sc. in applied chemistry (2016) from University of Calcutta (India), and M.Tech. in materials science and engineering (2018) from Indian Institute of Technology, Kanpur (India). His current research is focused on the cell–matrix interaction and 3D bioprinting on hydrogel-based bioink.



Bikramjit Basu has been serving on the faculty of Indian Institute of Science, Bangalore, since 2011. He is currently a Professor at Materials Research Center with joint appointment at Center for BioSystems

Science and Engineering. After PhD from Katholieke Universiteit Leuven, Belgium, he was on the faculty of Indian Institute of Technology Kanpur during 2001–2011. He is an elected fellow of the American Ceramic Society, Indian National Academy of Engineering, National Academy of Science, India; National Academy of Medical Sciences, American Institute of Medical and Biological Engineering and Institute of Materials, Minerals & Mining (UK). He is a recipient of the highest award for a scientist in India, the Shanti Swarup Bhatnagar Award, from the Govt. of India. He is currently leading India's largest Translational Center of Excellence on biomaterials for orthopaedic and dental applications, with an interdisciplinary team of 50 researchers, clinicians, and companies.